2022

Interconnection and damping assignment passivity-based non-linear observer control for efficiency maximization of permanent magnet synchronous motor

Youcef Belkhier

Abelyazid Achour

Miroslav Bures

See next page for additional authors

Funder: European Union; Enterprise Ireland; National Research and Development Agency of Chile (ANID)

Authors

Youcef Belkhier, Abelyazid Achour, Miroslav Bures, Nasim Ullah, Mohit Bajaj, Hossam Zawbaa, and Salah Kamel

Energy Reports 8 (2022) 1350–1361

Contents lists available at ScienceDirect

Energy Reports

journal homepage: www.elsevier.com/locate/egyr

Research paper

Interconnection and damping assignment passivity-based non-linear observer control for efficiency maximization of permanent magnet synchronous motor

Youcef Belkhier [a], Abdelyazid Achour [b], Miroslav Bures [a], Nasim Ullah [c], Mohit Bajaj [d], Hossam M. Zawbaa [e,f,*], Salah Kamel [g]

[a] Department of Computer Science, Faculty of Electrical Engineering, Czech Technical University in Prague, Karlovo Namesti 13, 121 35 Praha 2, Czechia
[b] Laboratoire de Technologie Industrielle et de l'Information (LTII), Faculté de Technologie, Université de Bejaia, Bejaia 06000, Algeria
[c] Department of Computer Science, College of Computers and Information, Taif University, P.O. Box 11099, Taif 21944, Saudi Arabia
[d] Department of Electrical and Electronics Engineering, National Institute of Technology Delhi, New Delhi 110040, India
[e] Faculty of Computers and Artificial Intelligence, Beni-Suef University, Beni-Suef, Egypt
[f] Technological University Dublin, Dublin, Ireland
[g] Electrical Engineering Department, Faculty of Engineering, Aswan University, 81542 Aswan, Egypt

ARTICLE INFO

Article history:
Received 11 October 2021
Received in revised form 25 November 2021
Accepted 18 December 2021
Available online xxxx

Keywords:
Passivity-based control
Interconnection and damping assignment
Permanent magnet synchronous motor
Non-linear observer

ABSTRACT

The permanent magnet synchronous motor (PMSM) has several advantages over the DC motor and is gradually replacing it in the industry. The dynamics of the PMSM are described by non-linear equations; it is sensitive to unknown external disturbances (load), and its characteristics vary over time. All of these restrictions complicate the control task. Non-linear controls are required to adjust for non-linearities and the drawbacks mentioned above. This paper investigates an interconnection and damping assignment (IDA) passivity-based control (PBC) combined with a non-linear observer approach for the PMSM using the model represented in the dq-frame. The IDA-PBC approach has the inherent benefit of not canceling non-linear features but compensating them in a damped manner. The suggested PBC is in charge of creating the intended dynamic of the system, while the non-linear observer is in charge of reconstructing the recorded signals in order to compel the PMSM to track speed. The primary objective of this study is to synthesize the controller while accounting for the whole dynamic of the PMSM and making the system passive. It is performed by restructuring the energy of the proposed strategy and introducing a damping component that addresses the non-linear elements in a damped instead of deleted way, so providing a duality concept between both the IDA-PBC and the observer There are three methods for computing IDA-PBC: parametric, nonparametric, and algebraic. The parameterized IDA-PBC method is used to control the speed of the PMSM. This method uses the energy function in parameterized closed-loop in terms of some functions depending on the system's state vector, such that the energy formation step is satisfied. Then, the original port-controlled Hamiltonian (PCH) dynamics in open-loop (OL) are equalized with the desired one in closed-loop (CL). The equalization process allows obtaining a set of solutions of the partial differential equations. The latter must be solved in terms of the parameters of the energy function of the closed-loop. Finally, the stability properties are studied using the Lyapunov theory. Generally, the proposed candidate offers high robustness, fast speed convergence, and high efficiency over the conventional benchmark strategies. The effectiveness of the proposed strategy is performed under extensive numerical investigation with MATLAB/Simulink software.

1. Introduction

Non-linear equations are commonly used to represent electrical machines. The inductances and coefficients of the dynamic equations, which are dependent on the rotor position and time, cause this non-linearity. By lowering the number of variables and

* Corresponding author at: Technological University Dublin, Dublin, Ireland.
E-mail addresses: youcef.belkhier@fel.cvut.cz (Y. Belkhier), abdelyazid.achour@univ-bejaia.dz (A. Achour), buresm3@fel.cvut.cz (M. Bures), nasimullah@tu.edu.sa (N. Ullah), mohitbajaj@nitdelhi.ac.in (M. Bajaj), hossam.zawbaa@gmail.com (H.M. Zawbaa), skamel@aswu.edu.eg (S. Kamel).

https://doi.org/10.1016/j.egyr.2021.12.057

Nomenclature and Abbreviations

PDE	Partial differential equations
PCE	Port-controlled Hamiltonian
PMSM	Permanent Magnet Synchronous Motor
PWM	Pulse width modulation
SMC	Sliding mode control
DO	Disturbance Observer
PBC	Passivity based control
EBC	Energy based control
FOC	Field oriented control
τ_L	Load torque
ω_m	The PMSM speed
CL	Closed loop
OL	Open loop
C_{em}	PMSG electromagnetic torque, N m
φ_f	Flux linkages due to the permanent magnets
L_{dq}	Induction matrix of the stator
f_{fv}	Coefficient of the viscous friction
J_m	Total inertia moment
$\mathcal{R}(x)$	The matrix of dissipation
$\mathcal{J}(x)$	The matrix of interconnection
$H(x)$	Total stored energy
x	The state vector
$H_a(x)$	Energy added
V_{dc}	Direct voltage in the DC grid, Volts
i_d, i_q v_d, v_q	Current and voltage components along d and q rotor axes respectively, A and Volts
ω	Electric pulsation
n_p	Pair pole number of the PMSM
R_s	Stator phase resistances, Ω
R_{dq}	Stator resistance matrix, Ω
$\hat{\omega}$, $\hat{\tau}_L$	Observed speed and load torque
l_1 and l_2	Observer gains
$\tilde{\omega}$	Speed observation error
$\tilde{\tau}_L$	Load torque observation error
λ	Tip speed ratio
ψ_d, ψ_q, ψ_f	Rotor flux components along d and q flux linkages vector

deleting the rotor position in the differential 'equations' coefficients, a change of variables is frequently utilized to simplify this dynamic model. The steady-state conditions, stability analysis, and control synthesis are significantly easier to determine in this scenario (Allouche et al., 2020; Zhao et al., 2021).

The PMSM has a stator similar to the stator of all three-phase electrical machines. The change of the rotor winding by permanent magnets brings a lot of simplicity, such as reducing the overall dimensions and easier modeling because the rotor dynamics are restricted to the flux created by the permanent magnets. Because of its appealing qualities in terms of efficiency, power density, torque-to-inertia ratio, and dependability, the PMSM is an enticing alternative for several high-precision applications. Nevertheless, the 'PMSM's differential equations and time-varying features make the controller computing difficult (Urbanski and Janiszewski, 2019; Li et al., 2020). Several research works dedicated to the control of PMSM have appeared in the literature and the industry. According to recent research, the most commonly utilized control systems that have shown to be very common and useful can be categorized into two types: linear and non-linear controller-based approaches. The proportional–integral (PI) controller is among the most popular linear methodologies, and it provides a continuous reference and is then digitized by pulse width modulation (PWM) (Urbanski and Janiszewski, 2019). In addition, common techniques include deadbeat (Scarcella et al., 2017) and state feedback control (Apte et al., 2020). The only thing both solutions have in common is that they both necessitate the use of a PWM. Meanwhile, the majority of linear control systems are built, assuming that the system will be located in a linear region. Several other limitations and non-linearities in drive systems and real power electronics were overlooked (Alfehaid et al., 2021).

There have been numerous non-linear techniques of controlling permanent magnet synchronous machines examined. A direct speed control combined with a state-dependent Riccati equation is proposed in Šmídl et al. (2018), where the current amplitude and the field-weakening curve are both constrained explicitly. The issue is phrased as quadratic programming with a quadratic constraint since the cost-to-go function for the controller is known. To increase the disturbance rejection ability and dynamic performance of PMSM drive systems, a novel sliding-mode-based extended state observer is presented in Xu et al. (2021). First, for better comparison, an extended state observer based on the fast terminal sliding-mode control approach is proposed, which may increase the resilience against load disturbances, finite time integration, and significant minimization of the chattering problem. An improved non-linear flux observer is presented in Xu et al. (2019). The rotor location estimate approach based on PMSM rotor flux monitoring is investigated first. Furthermore, the constraints of classic rotor flux estimators, such as pure integrator saturation, phase shift, and amplitude attenuation of a low-pass filter, are investigated. An Adaptive fuzzy controller is investigated in Mani et al. (2019). Through the use of effective Takagi–Sugeno fuzzy membership criteria, the non-linear PMSM model is turned into corresponding linear submodels. Then, to control the considered PMSM, a unique automated (adaptive) controller is constructed in conjunction with a fractional sliding surface that includes an integral term. In Junejo et al. (2020), an adaptive speed controller-based sliding mode control (SMC) is proposed. Nonlinear Disturbance Observer (DO)-Based SMC approach is developed in Nguyen et al. (2020). The model predictive controller is depicted in Niu et al. (2020). The DO-based control approach is the better option between these approaches for improving the drive 'systems' disturbance rejection efficiency. However, it has poor load disturbance rejection and dynamic control capabilities. Furthermore, in reality, the sliding mode causes high frequency changing, sometimes known as "chattering". These switches have the potential to elicit undesirable behaviors that might destabilize, degrade, or even break the system under investigation. Moreover, as mentioned in Yang et al. (2018), the majority of these controls are signal-based and do not take into account the physical structure of the synchronous machine during the controller design. This work proposes a novel control method based on the passivity concepts that track velocity and maintains this one operating at the optimal torque. The inherent advantages of the passivity-based control (PBC) method, also called Energy-based control (EBC) are that the non-linear properties are not canceled but compensated in a damped way. PBC designs aim to rearrange the system's natural energy and inject the necessary dampening in efforts to realize the regulation goal. The increased robustness characteristics and lack of (controller calculation) discontinuities, which result from the avoidance of system non-linearities elimination, are obvious advantages of this approach (Nicklasson et al., 1994, 1997).

Several studies on passivity control devoted to the PMSM have appeared in the literature and industry. In Achour et al. (2009), a

passivity-based current control is proposed where the magnetic fluxes are used as the state variables instead of the currents for a PMSM. The passivity-based speed controller is investigated in Ramirez-Leyva et al. (2013). A sampled-data interconnection and the damping assignment PBC (IDA-PBC) approach is investigated in Khanchoul et al. (2014). An IDA technique has been integrated with a passivity-based active disturbance rejection control (Wang et al., 2018). In Liu et al. (2019), a PBC combined with a speed control method and Disturbance Observer is proposed. The present paper investigates a new IDA-PBC combined with a non-linear observer approach, with simple structure and simple mathematical calculation, investigated and simulated the PMSM. The main idea of the IDA-PBC is a technique that regulates the behavior of the non-linear systems by assigning a desired port-controlled Hamiltonian (PCH) structure to the closed-loop. The key issue is identifying the workless force terms in the process model that do not affect its dynamics.

Contrary to the "classical" PBC proposed in Achour et al. (2009), Ramirez-Leyva et al. (2013), Khanchoul et al. (2014) and Wang et al. (2018), the IDA-PBC methodology is based on energy-shaping and passivation principles but focused on the interconnection and damping structures of the system (Ortega et al., 2002; Ortega and Canseco, 2004). The proposed PBC is responsible for designing the system's desired dynamic, while the non-linear observer is responsible for reconstructing the measured signals to force the PMSM to track speed. The main objective of this study is to construct the control system simultaneously accounting for the whole dynamic of the PMSM and making the system passive. It is accomplished by rearranging the energy of the proposed IDA-PBC and inserting a damping factor that compensates the non-linear terms in a damped rather than canceled manner, establishing a duality idea between the observer and the IDA-PBC.

The IDA-PBC may be computed in three ways: parametrically, nonparametrically, and algebraically. To regulate the speed of the PMSM, the parameterized IDA-PBC technique is employed. This technique employs the energy function in a parameterized closed-loop in terms of certain functions depending on the system's state vector, therefore satisfying the energy creation step. The intended PCH dynamics are then equalized with the original PCH dynamics (in open-loop) (in closed-loop). The equalization procedure yields a collection of partial differential equation solutions (PDE). The latter must be solved in terms of the parameters of the closed-energy loop's function. Finally, the Lyapunov theory is used to investigate the stability qualities. A comparison of the proposed IDA-PBC and the conventional field-oriented control (FOC) is undertaken, revealing that the suggested IDA-PBC provides quick convergence, good stability, and the lowest tracking errors. The main originality and contribution of the present work over the related papers in the literature are summarized as given below:

- A new IDA-PBC combined with a non-linear observer approach, with simple structure and simple mathematical calculation, is investigated for optimal performance of a PMSM. Although duality is a hallmark of linear systems, the crucial feature of this technique is the duality created between the controller synthesis approach and that of the observer.
- The essential characteristic of this approach is the extremely reduced number of the fixed gains used by the proposed strategy, which avoids its sensitivity to parameter uncertainties, which highly improves the system's robustness property and global stability to the load and relative uncertainties on all engine parameters. This characteristic is ensured by injecting large gains with respect to the nominal values of the system variables.
- Extensive numerical investigations are made to demonstrate the robustness of the proposed approach against parameter changes and external disturbances.
- The closed-loop system is globally and asymptotically stable, and dynamic errors converge exponentially to zero, with the rate controlled by the amortization term.

The present form organizes the present paper: in Section 2, the system description is established. Sections 3 and 4 deal with the proposed strategy design procedure. Section 5 deals with the extensive numerical investigation of the proposed strategy. Finally, Section 6 deals with the main conclusions of the present paper.

2. PM synchronous motor description

To design the proposed strategy, the dq-model of the PMSM is considered, expressed as (Achour et al., 2009):

$$v_{dq} = R_{dq} i_{dq} + L_{dq} \dot{i}_{dq} + p\omega \mathfrak{I} L_{dq} i_{dq} + p\omega \mathfrak{I} \psi_f \tag{1}$$

$$J_m \dot{\omega}_m = \tau_L - f_{fv} \omega_m - C_{em} \tag{2}$$

$$C_{em} = \frac{3}{2} n_p \left(\left(L_d - L_q \right) i_d i_q + \varphi_f i_q \right) \tag{3}$$

where $\mathrm{R_{dq}} = \begin{bmatrix} \mathrm{R_s} & 0 \\ 0 & \mathrm{R_s} \end{bmatrix}$ denotes the stator resistance matrix, f_{fv} represents the coefficient of the viscous friction, $\psi_f = \begin{bmatrix} \varphi_f \\ 0 \end{bmatrix}$ is the flux linkages vector, C_{em} represents the electromagnetic torque, $\mathrm{L_{dq}} = \begin{bmatrix} \mathrm{L_d} & 0 \\ 0 & \mathrm{L_q} \end{bmatrix}$ denotes the induction matrix of the stator, J_m represents the total inertia moment, $\mathrm{v_{dq}} = \begin{bmatrix} \mathrm{v_d} \\ \mathrm{v_q} \end{bmatrix}$ denotes voltage stator vector, $\mathrm{i_{dq}} = \begin{bmatrix} \mathrm{i_d} \\ \mathrm{i_q} \end{bmatrix}$ denotes the stator current vector, and ω_m denotes the PMSM speed. φ_f are the flux linkages due to the permanent magnets, n_p is the number of pole-pairs, $\mathfrak{I} = \begin{bmatrix} 0 & -1 \\ 1 & 0 \end{bmatrix}$, and τ_L is the load torque.

3. IDA-PBC theory and design procedure

The IDA-PBC approach was proposed in refs. (Ortega et al., 2002; Ortega and Canseco, 2004), to control physical systems modeled by a PCH model, which are described as follow:

$$\begin{cases} \dot{x} = \left[\mathcal{J}(x) - \mathcal{R}(x) \right] \dfrac{\partial H}{\partial x}(x) + g u \\ y = g^T(x) \dfrac{\partial H}{\partial x}(x) \end{cases} \tag{4}$$

where, $H(x) : \mathfrak{R}^n \rightarrow \mathfrak{R}^+$ is the total stored energy, $x \in \mathfrak{R}^n$ represent the state vector, $u \in \mathfrak{R}^m, m < n$ is the controller action, the product of u and $y \in \mathfrak{R}^m$ has units power, and $\mathcal{J}(x) = -\mathcal{J}^T(x)$, $\mathcal{R}(x) = \mathcal{R}^T(x) \geq 0$ are the matrix of interconnection and dissipation, respectively. The main difference between classical PBC and IDA-PBC is that in the latter, the energy function of the closed-loop is obtained (not proposed) through the solution of a partial derivative equation (PDE), which is the result of matrix selection. It is well known that solving a PDE equation is generally difficult. However, a judicious selection of the desired matrices by considering the system's physical characteristics can help obtain the solution of the corresponding PDE (Ortega et al., 2002). The

IDA-PBC design proceeds as: first, we select the desired storage function by fixing the desired structure of the interconnection and damping matrices. Second, we solve the PDE based on the chosen matrices. Finally, find a controller u which makes the closed-loop dynamics as a PCH system with dissipation.

3.1. Permanent magnet synchronous motor PCH structure

The first step in the IDA-PBC calculation is the design of the PCH structure of the PMSM. Considering the PMSM model given in Section 2, where the viscous friction coefficient f_{fv} is neglected. The following equations are formulated:

$$\begin{cases} \dfrac{d\left(L_d i_d\right)}{dt} = -R_s i_d + \omega L_q i_q + v_d \\ \dfrac{d\left(L_q i_q\right)}{dt} = -\omega L_d i_d - R_s i_q - \omega\varphi_f + v_q \\ \dfrac{d}{dt}\left(\dfrac{J_m}{n_p}\left(n_p\omega\right)\right) = -\left(n_p L_q i_q\right) i_d + \left(n_p L_d i_d + n_p\varphi_f\right) i_q - \tau_L \end{cases} \tag{5}$$

All parameters of the model (5) are defined in Section 2. The energy function in open-loop (OL) is given by the following relation (Ortega et al., 2002):

$$H(x) = \frac{1}{2}\left(\frac{1}{L_d}x_1^2 + \frac{1}{L_q}x_2^2 + \frac{n_p}{J_m}x_3^2\right) \tag{6}$$

where x is the state vector defined by the following vector:

$$x = \begin{bmatrix} x_1 & x_2 & x_3 \end{bmatrix}^T = \begin{bmatrix} L_d i_d & L_q i_q & \left(J_m/n_p\right)\omega \end{bmatrix}^T \tag{7}$$

The PCH model of the PMSM has the following form (Ortega and Canseco, 2004):

$$\begin{cases} \dot{x}(t) = [J(x) - R(x)]\nabla H(x) + g(x)u(t) + \xi \\ y(t) = g^T(x)\nabla H(x) \end{cases} \tag{8}$$

It is calculated using Eqs. (5)–(7) which yields the following expressions:

$$J(x) = \begin{bmatrix} 0 & 0 & x_2 \\ 0 & 0 & -\left(x_1 + \varphi_f\right) \\ -x_2 & \left(x_1 + \varphi_f\right) & 0 \end{bmatrix},$$

$$R(x) = \begin{bmatrix} R_s & 0 & 0 \\ 0 & R_s & 0 \\ 0 & 0 & 0 \end{bmatrix},\ g(x) = \begin{bmatrix} 1 & 0 \\ 0 & 1 \\ 0 & 0 \end{bmatrix},\ \xi = \begin{bmatrix} 0 \\ 0 \\ -\dfrac{\tau_L}{n_p} \end{bmatrix}$$

$$u = \begin{bmatrix} v_d \\ v_q \end{bmatrix},\ \nabla H = \begin{bmatrix} \dfrac{\partial H}{\partial x_1}(x) \\ \dfrac{\partial H}{\partial x_2}(x) \\ \dfrac{\partial H}{\partial x_3}(x) \end{bmatrix} = \begin{bmatrix} x_1 \\ x_2 \\ x_3 \end{bmatrix} \text{ and } y = \begin{bmatrix} y_1 \\ y_2 \\ y_3 \end{bmatrix} = \begin{bmatrix} x_1 \\ x_2 \\ x_3 \end{bmatrix}$$

where, $H(x) \geq 0$, $J(x) = -J^T(x)$ et $R(x) = R^T(x) \geq 0$, $J(x)$ is the matrix of interconnections between states, and $R(x)$ is the matrix of natural damping of the system.

3.2. Proposed control design

The objective is to calculate the IDA-BC defined by the following vector:

$$u = \begin{bmatrix} v_d & v_q \end{bmatrix}^T = \beta(x) \tag{9}$$

which provides the system with a new PCH structure in the closed-loop (CL) of the form:

$$\begin{cases} \dot{x} = [J_d(x) - R_d(x)]\nabla H_d \\ y = g^T(x)\nabla H_d \end{cases} \tag{10}$$

This stabilizes x around the equilibrium point x^*, corresponding to the minimum of $H_d(x)$, that is:

$$\begin{cases} \dfrac{\partial H_d}{\partial x}(x_*) = 0_{3\times 1} \\ \dfrac{\partial^2 H_d}{\partial x^2}(x_*) \geq 0 \end{cases} \tag{11}$$

The new matrices of the PCH model (11) are chosen, respecting the physical constraints of the PMSM and the following conditions:

$$\begin{cases} J_d(x) = -J_d^T(x) \\ R_d(x) = R_d^T(x) \geq 0 \\ H_d(x) > 0, \forall x \neq \underline{0} \end{cases} \tag{12}$$

It is necessary that $H_d(x)$ be compatible with this PCH structure in CL. One of the consequences of the PCH structure is the linearity of the relations between the system matrices in CL and those in OL, through the controller:

$$J_d(x) = J(x) + J_a(x) \tag{13}$$

$$R_d(x) = R(x) + R_a(x) \tag{14}$$

$$H_d(x) = H(x) + H_a(x) \tag{15}$$

where $J_a(x)$, $R_a(x)$, and $H_a(x)$ are, respectively, the interconnection matrix, damping matrix, and energy added by the controller.

Equalizing (10) and (8) taking into account (13)–(15) gives the following PDE:

$$[J_d(x) - R_d(x)]\frac{\partial H_a}{\partial x}(x) = [J_a(x) - R_a(x)]\frac{\partial H}{\partial x}(x) + g(x)\beta(x) + \xi \tag{16}$$

The solutions of (16) are $\nabla H_a = \frac{\partial H_a}{\partial x}(x)$ et $\beta(x)$.

The necessary condition for the solvability of (16) is that:

$$\frac{\partial^2 H_a}{\partial x^2}(x) = \left(\frac{\partial^2 H_a}{\partial x^2}(x)\right)^T \tag{17}$$

3.3. J_d et R_d matrices selection

The objective of the control is to stabilize the desired equilibrium x^* by modifying the desired energy function through new structures of internal interconnection, damping, and closed-loop control PCH. The adequate choice of the desired interconnection and damping matrices is a key step for the success of the IDA-PBC design (Ortega et al., 2002; Ortega and Canseco, 2004). The choice of the interconnection and damping matrices is conditioned by the physical constraints of the PMSM and the condition (11). The nature of the solutions ∇H_a et $\beta(x)$ hence the energy $R(x)$, and the performance of the IDA-PBC depend on this calculation. A simple choice of the matrices $J_d(x)$ and $R_d(x)$ is to make them equal to those of the system in OL, i.e., $J(x)$ and $R(x)$. This choice allows defining the IDA-PBC with natural interconnection. Thus, the matrices of the controller are:

$$J_a(x) = R_a(x) = 0_{3\times 3} \tag{18}$$

In CL, the following matrices are deduced:

$$J_d(x) = J(x) = \begin{bmatrix} 0 & 0 & x_2 \\ 0 & 0 & -\left(x_1 + \varphi_f\right) \\ -x_2 & \left(x_1 + \varphi_f\right) & 0 \end{bmatrix} \tag{19}$$

$$R_d(x) = R(x) = \begin{bmatrix} R_s & 0 & 0 \\ 0 & R_s & 0 \\ 0 & 0 & 0 \end{bmatrix} \tag{20}$$

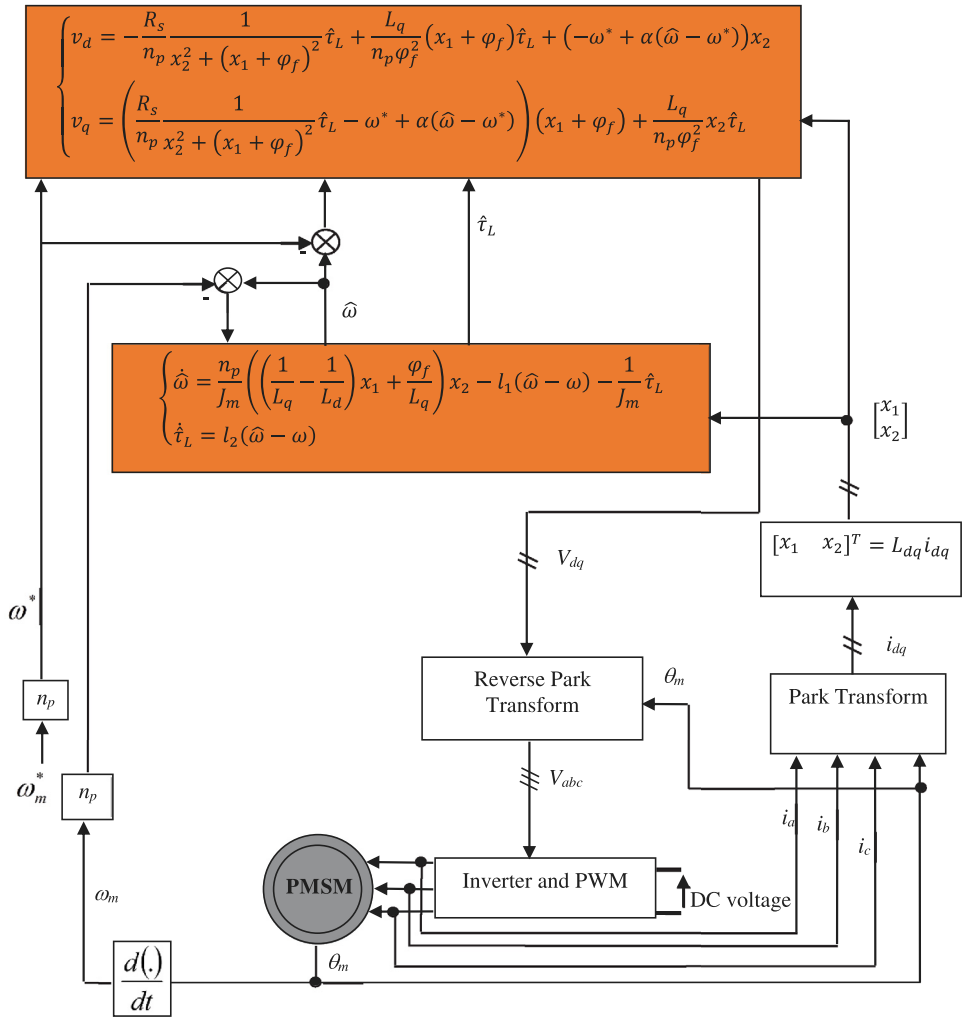

Fig. 1. Overall diagram of the IDA-PBC with speed and load torque observer for PMSM speed control.

The PCH model in CL is completely defined after $H_a()$ calculation.

3.4. Solution of the partial derivative equation

Taking into account (17), Eq. (15) is written:

$$[J(x) - R(x)]\frac{\partial H_a}{\partial x}(x) = g(x)\beta(x) + \xi \tag{21}$$

The voltage controller u of the PMSM can be obtained using the following expression (Ortega et al., 2002):

$$u = \left[g^T(x)g(x)\right]^{-1} g^T(x)\left\{[J_d(x) - R_d(x)]\nabla H_d - f(x)\right\} \tag{22}$$

Using Eqs. (21) and (22), it yields the following expressions for the control signals:

$$\begin{cases} v_d = -R_s\dfrac{\partial H_a}{\partial x_1}(x) + x_2\dfrac{\partial H_a}{\partial x_3}(x) \\ v_q = -R_s\dfrac{\partial H_a}{\partial x_2}(x) - (x_1+\varphi_f)\dfrac{\partial H_a}{\partial x_3}(x) \end{cases} \tag{23}$$

$$-x_2\frac{\partial H_a}{\partial x_1}(x) + (x_1+\varphi_f)\frac{\partial H_a}{\partial x_2}(x) = -\frac{\tau_L}{n_p} \tag{24}$$

The resolution of the PDE (24) gives $H_a(x)$. Thus, the explicit expressions (23) of the control signals are computed. The solution of (24) is realized by the function "solver symbolic" of MATLAB software, and the following general solution is obtained:

$$H_a(x) = \frac{\tau_L}{n_p}arctan\left(\frac{x_1+\varphi_f}{x_2}\right) + F\left(x_2^2 + x_1^2 + 2\varphi_f x_1\right) + h(x_3) \tag{25}$$

where F and h are two differentiable functions to be determined. To do this, we must first determine the desired equilibrium point x*.

3.5. Desired equilibrium point x^* computation

Our goal is to control the mechanical speed ω_m. Then the desired state x_3^* is calculated according to the set value ω_m^* and is calculated by the following equation:

$$x_3^* = J_m\omega^* \tag{26}$$

The PMSM operates at maximum torque if the desired forward current i_d^* in frame dq is zero. According to (7), $x_1 = L_d i_d$, therefore:

$$x_1^* = 0 \tag{27}$$

At the desired equilibrium point x^*, the third equation of (3) (i.e. the mechanical equation of the PMSM) is written:

$$n_p\varphi_f i_q^* - \tau_L = 0 \tag{28}$$

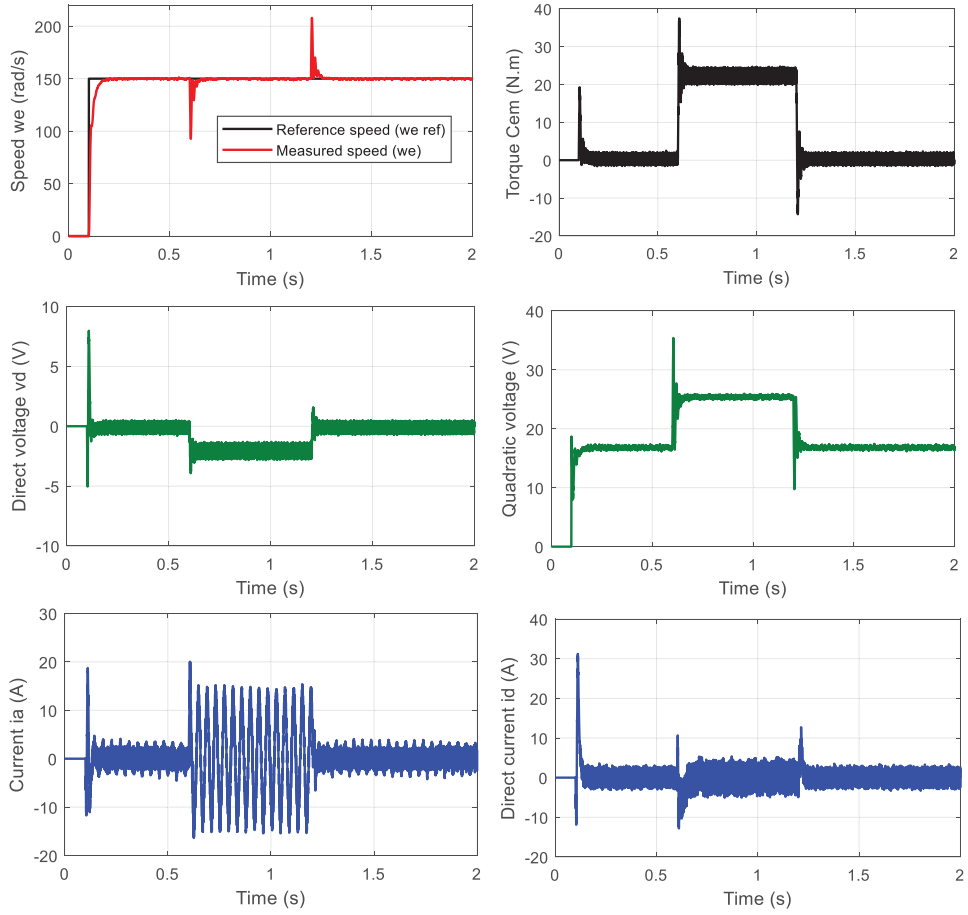

Fig. 2. Responses of the PMSM for a step of $\omega^* = 150$ rad/s with a load torque of 22 N m between 0.6 s and 1.2 s.

From (7) and (28), the desired value x_2^* is given by the following relation:

$$x_2^* = \frac{L_q}{n_p \varphi_f} \tau_L \tag{29}$$

Thus, the desired equilibrium points x^* is given by the following vector:

$$x^* = \begin{bmatrix} 0 & \frac{L_q}{n_p \varphi_f} \tau_L & J_m \omega^* \end{bmatrix}^T \tag{30}$$

3.6. Determination of the functions F and h

The functions F and h are determined by respecting the following conditions:

$$\begin{cases} \dfrac{\partial H_a}{\partial x}(x_*) = -\dfrac{\partial H}{\partial x}(x_*) \\ \dfrac{\partial^2 H_a}{\partial x^2}(x_*) > -\dfrac{\partial^2 H}{\partial x^2}(x_*) \end{cases} \tag{31}$$

where conditions (31) are deduced using relations (11) and (15).

Since, $\partial H_a / \partial x_3$ depends only on x_3, then, using the first equation of (31) and the expression (6), a simple choice of $h(x_3)$ is:

$$h(x_3) = -\omega^* e_3 + \frac{\alpha}{2} e_3^2 \tag{32}$$

where, $e_3 = x_3 - x_3^*$ and α is the gain to be determined.

Consider the function $f(z)$ defined by the following relation:

$$f(z) = \partial F(z) / \partial z \tag{33}$$

with:

$$z(x) = x_2^2 + x_1^2 + 2\varphi_f x_1 \tag{34}$$

At the desired equilibrium point x^* and using the conditions (31), the following relationships are obtained:

$$\begin{cases} f(\bar{z}) = -\dfrac{1}{2L_q} \dfrac{\bar{z}}{\bar{z} + \varphi_f^2} \\ \dfrac{\partial f}{\partial z}(\bar{z}) > \dfrac{1}{4L_q} \dfrac{\bar{z} - \varphi_f^2}{\left(\bar{z} + \varphi_f^2\right)^2} \end{cases} \tag{35}$$

where,

$$\bar{z} = \tau_L \tag{36}$$

Conditions (35) are satisfied if the following expression for $f(z)$ is chosen as:

$$f(z) = -\frac{1}{2L_q} \frac{\bar{z}}{z + \varphi_f^2} \tag{37}$$

3.7. Gradient calculation ∇H_a

The expression of ∇H_a is obtained, using the relation (26):

$$\nabla H_a = \begin{bmatrix} \dfrac{\partial H_a}{\partial x_1}(x) \\ \dfrac{\partial H_a}{\partial x_2}(x) \\ \dfrac{\partial H_a}{\partial x_3}(x) \end{bmatrix}$$

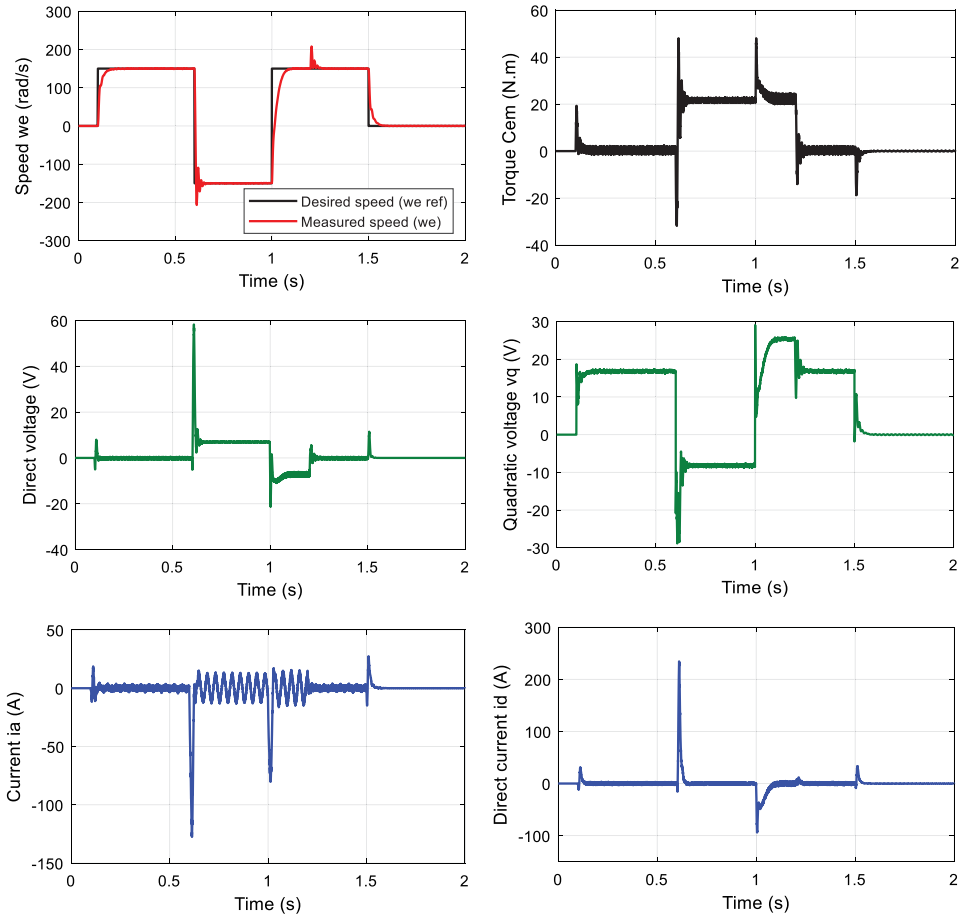

Fig. 3. PMSM simulation results for a ±150 rad/s set point with a load torque of 22 N m between 0.6 s and 1.2 s.

$$= \begin{bmatrix} \frac{\tau_L}{n_p} \frac{\partial\left(\arctan\left(\frac{x_1+\varphi_f}{x_2}\right)\right)}{\partial\left(\frac{x_1+\varphi_f}{x_2}\right)} \frac{\partial\left(\frac{x_1+\varphi_f}{x_2}\right)}{\partial x_1} + \frac{\partial F\left(x_2^2+x_1^2+2\varphi_f x_1\right)}{\partial\left(x_2^2+x_1^2+2\varphi_f x_1\right)} \frac{\partial\left(x_2^2+x_1^2+2\varphi_f x_1\right)}{\partial x_1} \\ \frac{\tau_L}{n_p} \frac{\partial\left(\arctan\left(\frac{x_1+\varphi_f}{x_2}\right)\right)}{\partial\left(\frac{x_1+\varphi_f}{x_2}\right)} \frac{\partial\left(\frac{x_1+\varphi_f}{x_2}\right)}{\partial x_2} + \frac{\partial F\left(x_2^2+x_1^2+2\varphi_f x_1\right)}{\partial\left(x_2^2+x_1^2+2\varphi_f x_1\right)} \frac{\partial\left(x_2^2+x_1^2+2\varphi_f x_1\right)}{\partial x_2} \\ \frac{h(x_3)}{\partial x_3} \end{bmatrix} \tag{38}$$

Using (35), (36), and (38), the following vector is obtained:

$$\nabla H_a = \begin{bmatrix} \frac{\tau_L}{n_p} \frac{1}{x_2^2+\left(x_1+\varphi_f\right)^2} \left(x_2 - \frac{L_q \tau_L}{n_p \varphi_f^2}\left(x_1+\varphi_f\right)\right) \\ -\frac{\tau_L}{n_p} \frac{1}{x_2^2+\left(x_1+\varphi_f\right)^2} \left(\frac{L_q \tau_L}{n_p \varphi_f^2} x_2 + \left(x_1+\varphi_f\right)\right) \\ -\omega^* + \alpha e_3 \end{bmatrix} \tag{39}$$

Remark 1. The control signal expressions vd and vq have the denominator, "$x_2^2 + \left(x_1+\varphi_f\right)^2$", which depends on the states x_1 and x_2 because of the first two components ∇H_a. This can cause the signals to diverge. To overcome the singularity problem, the initial values $x_1(0)$ and $x_2(0)$ must satisfy the following condition:

$$x_2^2(0) + \left(x_1(0)+\varphi_f\right)^2 \geq \sigma_{AIA}, \text{ avec } \sigma_{AIA} > 0 \tag{40}$$

By replacing the components of the vector ∇H_a by their values in (24) and knowing that $\alpha > 0$, the following expressions for the control signals are deduced:

$$\begin{cases} v_d = -\frac{R_s}{n_p} \frac{1}{x_2^2+\left(x_1+\varphi_f\right)^2} \tau_L + \frac{L_q}{n_p \varphi_f^2}\left(x_1+\varphi_f\right)\tau_L \\ +\left(-\omega^* + \alpha\left(\omega-\omega^*\right)\right) x_2 \\ v_q = \left(\frac{R_s}{n_p} \frac{1}{x_2^2+\left(x_1+\varphi_f\right)^2} \tau_L - \omega^* + \alpha\left(\omega-\omega^*\right)\right)\left(x_1+\varphi_f\right) \\ +\frac{L_q}{n_p \varphi_f^2} x_2 \tau_L \end{cases} \tag{41}$$

It can be noticed that the calculation of the IDA-PBC and x_2^* of requires the measurement of the load torque τ_L. However, in practice, this quantity is unknown. This requires its estimation.

4. Load torque and speed observer synthesis

A non-linear observer of the load torque τ_L and the speed ω_m or the electric pulsation ω ($\omega = n_p \omega_m$) is synthesized. In practice, the velocity is deduced by differentiation of the mechanical position or by a velocity sensor. These methods result in a poor-quality signal due to measurement noise on the position or the speed (Belkhier et al., 2021).

Since the load's consequences are on the velocity error, then the dynamics of $\hat{\tau}_L$ depending on this quantity. The expression for the velocity estimator $\widehat{\omega}$ is determined using the PMSM mechanical equation, and we have the following dynamics for the

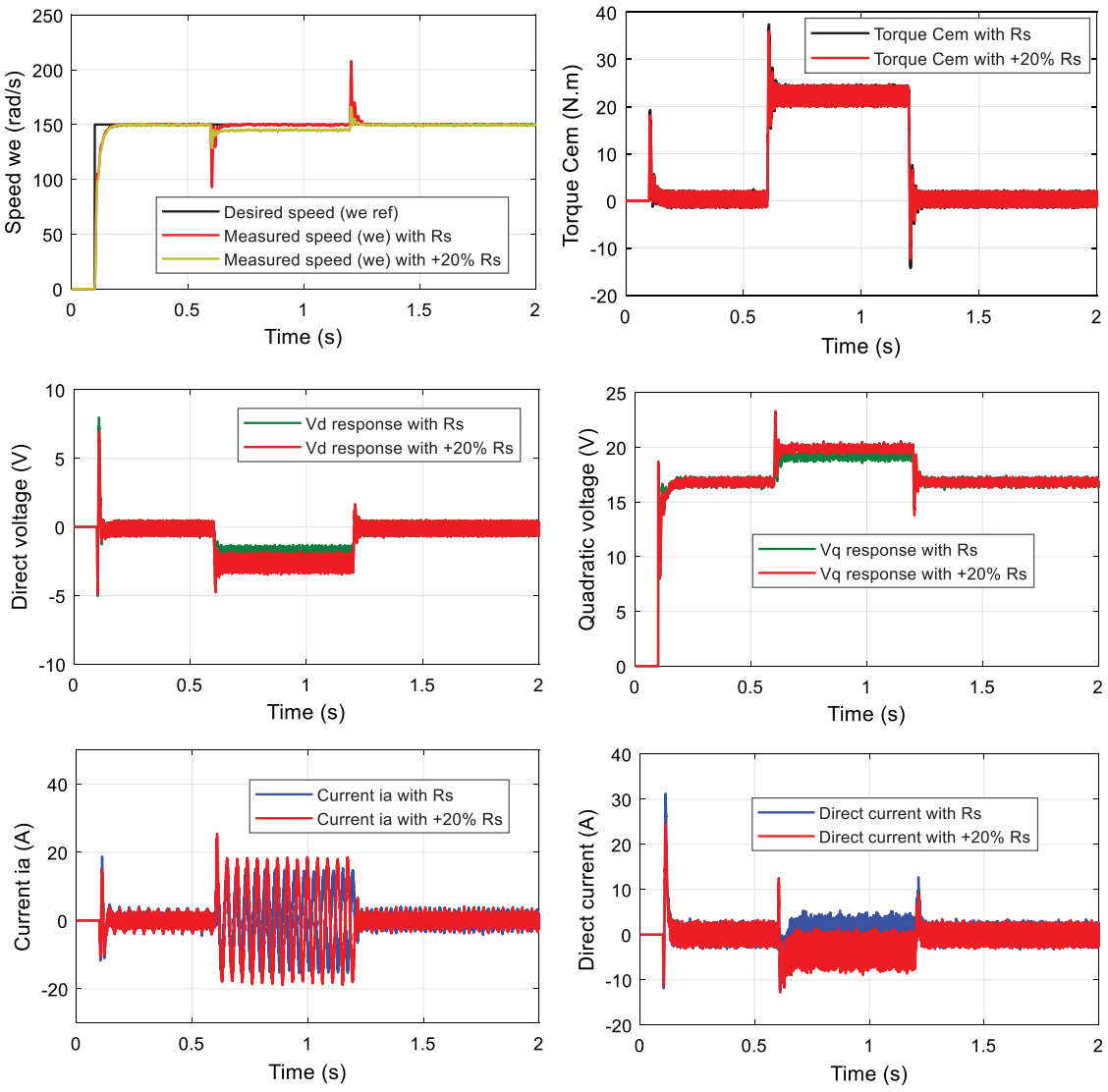

Fig. 4. Responses of the PMSM for a setpoint step of $\omega^* = 150$ rad/s with variations of +20% of the stator resistance *Rs* and a load torque of 22 N m between 0.6 s and 1.2 s.

observer of $(\widehat{\omega}, \hat{\tau}_L)$:

$$\begin{cases} \dot{\hat{\omega}} = \dfrac{n_p}{J_m}\left(\left(\dfrac{1}{L_q} - \dfrac{1}{L_d}\right)x_1 + \dfrac{\varphi_f}{L_q}\right)x_2 - l_1\left(\hat{\omega} - \omega\right) - \dfrac{1}{J_m}\hat{\tau}_L \\ \dot{\hat{\tau}}_L = l_2\left(\hat{\omega} - \omega\right) \end{cases} \tag{42}$$

with, l_1 and l_2 are gains to be determined, respecting the following conditions:

$$l_1, l_2 > 0 \tag{43}$$

Fig. 1 shows the block diagram of the IDA-PBC with speed and load torque observer.

4.1. Gains l_1 and l_2 computation

The design of the gains l_1 and l_2 of the observer is done in OL. Then, the first equation of (42) is subtracted from the third relation of (8) and knowing that:

$$\hat{\tau}_L = \tilde{\tau}_L + \tau_L \tag{44}$$

Assuming that τ_L is constant, the following dynamics of the estimation errors are deduced:

$$\begin{bmatrix} \dot{\tilde{\omega}} \\ \dot{\tilde{\tau}}_L \end{bmatrix} = \underbrace{\begin{bmatrix} -l_1 & -\dfrac{1}{J_m} \\ l_2 & 0 \end{bmatrix}}_{A_{obs}} \begin{bmatrix} \tilde{\omega} \\ \tilde{\tau}_L \end{bmatrix} \tag{45}$$

where the relations define the observation errors: $\tilde{\omega} = \hat{\omega} - \omega$ and $\tilde{\tau}_L = \hat{\tau}_L - \tau_L$.

The calculation of l_1 and l_2 is done by the method of pole placement of the A_{Obs} matrix. The Eq. (45) admits the following solution:

$$\begin{bmatrix} \tilde{\omega}(t) \\ \tilde{\tau}_L(t) \end{bmatrix} = \begin{bmatrix} \tilde{\omega}(0) \\ \tilde{\tau}_L(0) \end{bmatrix} e^{A_{Obs}t} \tag{46}$$

It is sufficient that A_{Obs} is positive for $\tilde{\omega}$ and $\tilde{\tau}_L$ to converge to zero.

4.2. Gains l_1 and l_2 computation

The Lyapunov theory performs the stability analysis. Then, the first step is to choose the following quadratic function:

$$V_{AIA}^{Obs}(x, \tilde{\omega}, \tilde{\tau}_L) = H_d(x) + \frac{1}{2}\begin{bmatrix} \tilde{\omega} & \tilde{\tau}_L \end{bmatrix} I_2 \begin{bmatrix} \tilde{\omega} & \tilde{\tau}_L \end{bmatrix}^T \tag{47}$$

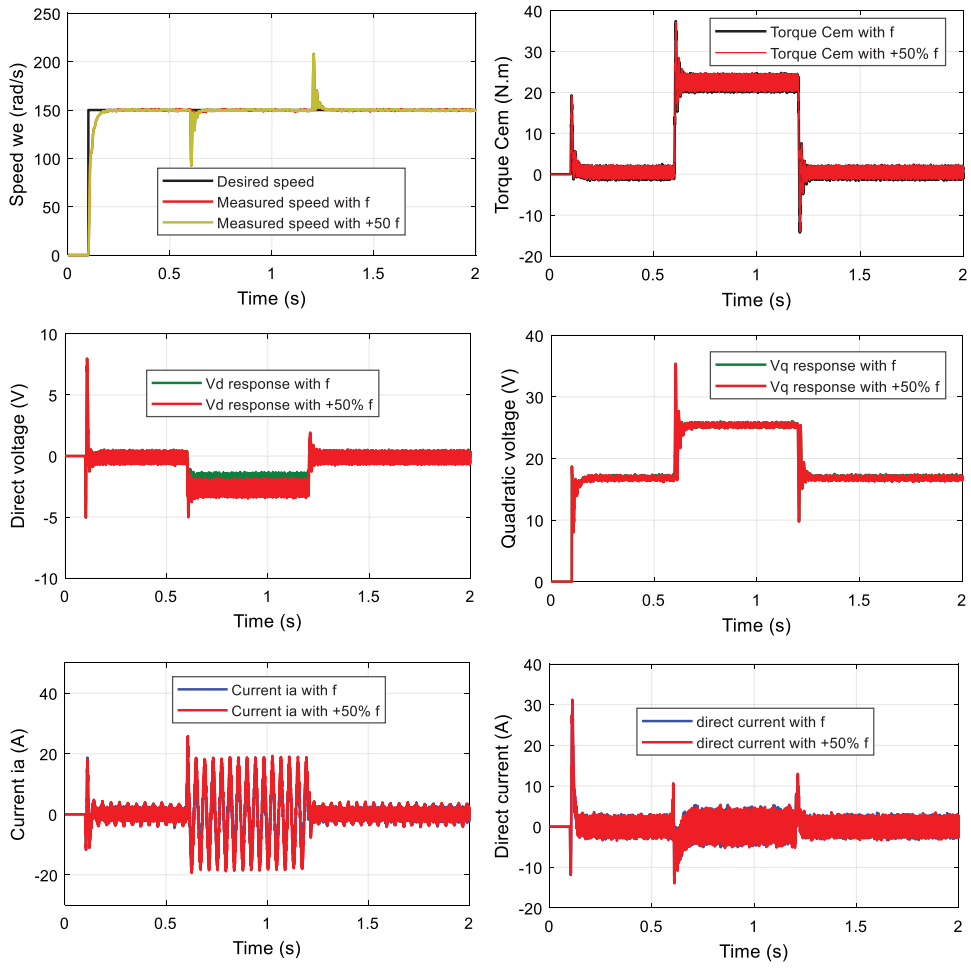

Fig. 5. Responses of the PMSM for a setpoint step of $\omega^* = 150$ rad/s with variations of +50% of the viscous friction coefficient f_{fv} and a torque load of 22 N m between 0.6 s and 1.2 s.

By deriving V_{AIA}^{Obs} with respect to time along the trajectories (13), (45), the following relation is obtained:

$$\dot{V}_{AIA}^{Obs}(x,\ \widetilde{\omega},\ \tilde{\tau}_L) = \dot{x} = -\nabla H_d^T R_d(x) \nabla H_d + \frac{1}{2}\begin{bmatrix}\widetilde{\omega} & \tilde{\tau}_L\end{bmatrix} A_{Obs} \begin{bmatrix}\widetilde{\omega} & \tilde{\tau}_L\end{bmatrix}^T \tag{48}$$

Eq. (48) is rearranged in the following compact form:

$$\dot{V}_{AIA}^{Obs}(x,\ \widetilde{\omega},\ \tilde{\tau}_L) = -\begin{bmatrix}\nabla H_d^T & \widetilde{\omega} & \tilde{\tau}_L\end{bmatrix} \underbrace{\begin{bmatrix} R_d(x) & 0_{3\times 2} \\ 0_{2\times 3} & -A_{Obs}\end{bmatrix}}_{A_{AIA}^{Obs}} \begin{bmatrix}\nabla H_d^T \\ \widetilde{\omega} \\ \tilde{\tau}_L\end{bmatrix} \tag{49}$$

It is sufficient that the matrix A_{AIA}^{Obs} is positive definite, i.e., with stable poles, for the equilibrium point $\begin{bmatrix}x & \widetilde{\omega} & \tilde{\tau}_L\end{bmatrix} = \begin{bmatrix}x^* & 0_{1\times 2}\end{bmatrix}$ to be stable, given that x^* cancels ∇H_d. This condition is verified because $R_d(x) = R(x)$ is a stable diagonal matrix, and the gains l_1 and l_2 are chosen so that $(-A_{Obs})$ is stable.

5. Simulation results

The IDA-PBC with electrical pulsation and load torque observer given by the relations (41)–(43) is validated by simulations. The parameters of the studied PMSM and the inverter are defined in Tables 1 and 2. The motor is powered by a voltage inverter controlled by the PWM technique.

Table 1
PMSM parameters.

PMSM parameter	Value
Rated speed [tr/min]	3000
Rated voltage [V]	310
Nominal torque [N m]	22
Rated current [A]	31
Number of pole pairs (p)	4
Inertia moment [kg m^2]	0.0048
Weight [kg]	25
Stator phase resistance Rs [Ω]	0.17377
Direct inductance Ld [mH]	0.8524
Quadratic inductance Lq [mH]	0.9515
Flux amplitude of the permanent magnets [Wb]	0.1112
Viscous friction coefficient [N m/rd/s]	0.0085

The controller gain α is determined by simulation tests and by respecting the stability condition $\alpha > 0$. The observer gains l_1 and l_2 are calculated by the pole placement method. The values used are: $\alpha = 10$, $l_1 = 80$, and $l_2 = 7.68$.

5.1. Performance analysis under fixed parameters

Fig. 2 represents the responses of the PMSM for a setpoint step of 150 rads/s with a load torque of 22 N m between 0.6 s and 1.2 s. It can be seen that the controller eliminates the effect of the load. Since the speed signal ω reaches its set point with a very short response time. The magnitude of the line current

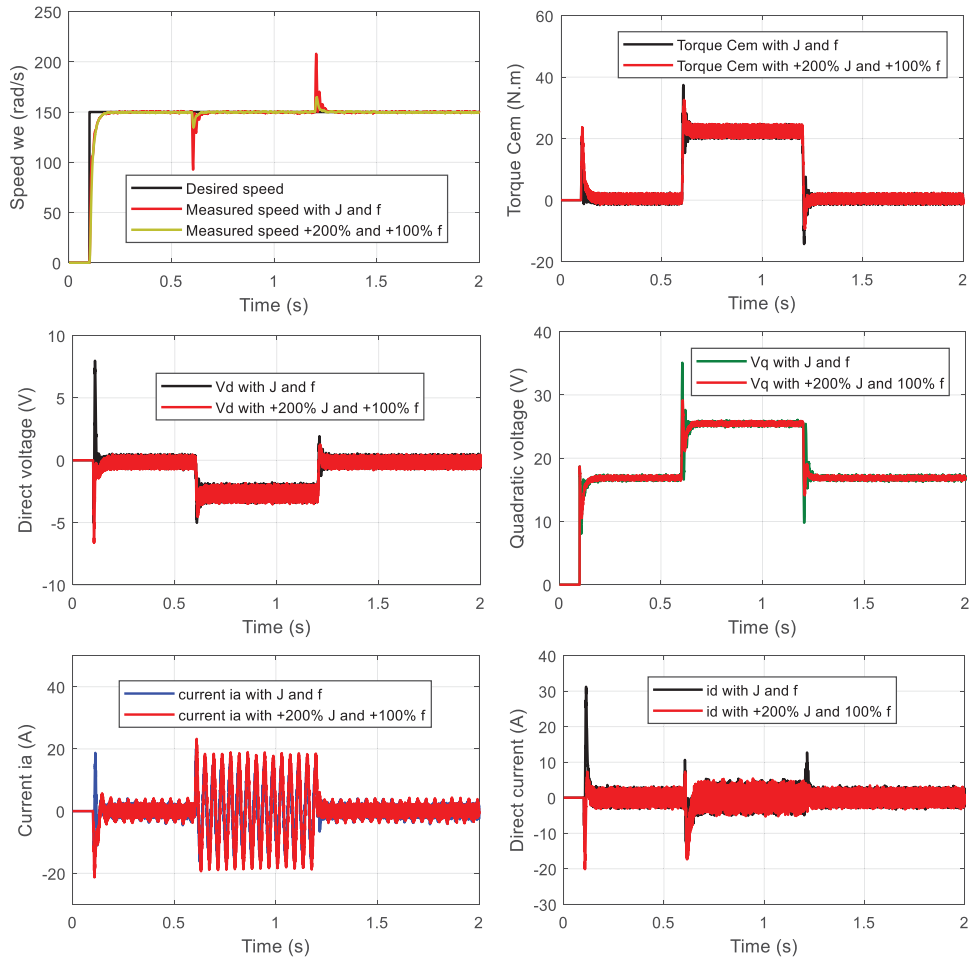

Fig. 6. PMSM responses for a setpoint step of $\omega^* = 150$ rad/s with simultaneous variations of $+100\%$ of f_{fv} and 200% of the moment of inertia J_m and a load of 22 N m between 0.6 s and 1.2 s.

Table 2
Inverter parameters.

Inverter parameter	Value
Inverter guard time [s]	0.00000325
PWM frequency [kHz]	10
Power supply voltage [V]	270
PWM control coefficient	0.9
Modulation index	21

is increased during the application of the load to provide the energy necessary to overcome the load and maintain the speed at its reference. The electromagnetic torque increases to a value corresponding to the load and friction. The control voltages v_{dq} at the output of the controller stabilize at finite and acceptable values. The direct current i_d is equal to its reference value which is zero. The oscillations in the signals are due to the motor supply inverter and the peaks due to the shape of the setpoint speed.

The results of the tests with a setpoint in the form of a ± 150 rad/s slot with a load of 22 N m between 0.6 s and 1.2 s are given in Fig. 3. It can be seen that the IDA-PBC with observer provides good performance, and all signals are stable. The oscillations and peaks are due to the causes already mentioned.

5.2. Robustness tests

The results of the robustness tests with respect to variations of $+20\%$ of the stator resistance R_s, $+50\%$ of the coefficient of viscous friction f_{fv}, and simultaneous variations of $+100\%$ of f_{fv} and $+200\%$ of the moment of inertia J_m are represented respectively by Figs. 4–6. A setpoint step of 150 rads/s is imposed with a load torque of 22 N m between 0.6 s and 1.2 s. We notice that the variations of R_s and f_{fv} have no effect on the system in CL. This justifies the elimination of f_{fv} in the PMSM model, used for the calculation of the IDA-PBC. The important variations of J_m generate peaks (bearable by the PMSM) at startup, signals i_d, i_q, v_d, and the electromagnetic torque $\tau_L = C_{em}$ to ensure the energy necessary to compensate these variations.

5.3. A comparative analysis

A comparative analysis of the proposed IDA-PBC and the conventional field-oriented control (FOC) (Zakharov and Minav, 2020) is performed in Fig. 7, which shows that the proposed IDA-PBC ensures fast convergence, high stability, and the lowest tracking errors as in (Fig. 7(a)) in comparison to the tested benchmark strategy FOC. Thus, from the previous results shown in Fig. 7, the proposed method validates the objective mentioned in the introduction part, which is regulation of the speed to its pre-fault value and to guarantee efficient, secure, and reliable power to the PMSM, indeed any possible disturbances related to the Electrical power

6. Conclusion

In this paper, a new IDA-PBC with speed and load observer using the PCH model based on the concept of passivity has been

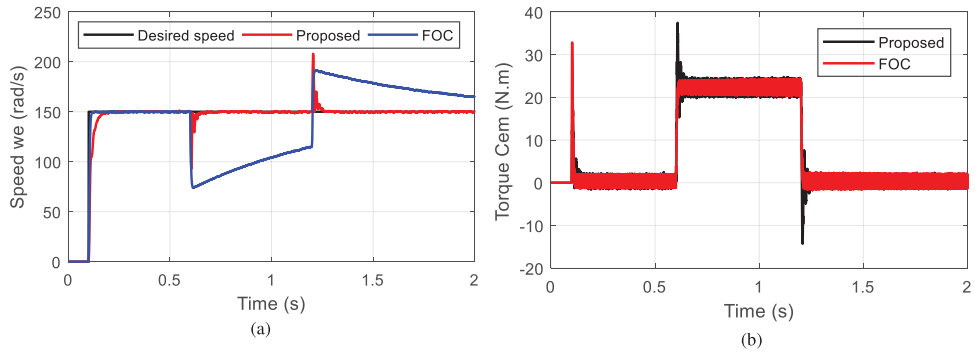

Fig. 7. Performance comparisons between the proposed IDA-PBC and the FOC. (a) speed response of both proposed control and FOC; (b) Cem response of both proposed control and FOC.

applied to the PMSM. This controller exploits the PCH model of the motor, which highlights three matrices: the interconnection matrix, which represents the internal energy exchange ports between the states of the PMSM, the damping matrix, which represents all the dissipation elements of the system, and the external interconnection matrix which represents the energy exchanges of the PMSM with its external environment. The particular characteristic of the IDA-PBC is the choice of the PCH structure in CL, then the energy function compatible with this model is determined. From the simulation tests, it is concluded that the IDA-PBC developed for the PMSM based on the concept of passivity has the following characteristics: The IDA-PBC with observer requires the determination of only three gains. Contrary to the classical controls, which uses more fixed gains. The primary objective of this study is to synthesize the controller while accounting for the whole dynamic of the PMSM and making the system passive. It is performed by reorganizing the proposed IDA-energy PBC's and introducing a damping component that compensates the non-linear terms in a damped rather than canceled way, so creating a duality concept between both the observer and the IDA-PBC. It is robust to the load and relative uncertainties on all engine parameters. This characteristic is ensured by injecting large gains with respect to the nominal values of the system variables. The system in CL is globally and asymptotically stable, and the dynamic errors converge exponentially to zero, the rate of which is controlled by the damping term. A comparison of the proposed IDA-PBC and the conventional FOC is undertaken, revealing that the suggested IDA-PBC provides quick convergence, good stability, and the lowest tracking errors.

CRediT authorship contribution statement

Youcef Belkhier: Data curation, Methodology, Software, Writing, Reviewing. **Abdelyazid Achour:** Data curation, Methodology, Software, Writing, Reviewing. **Miroslav Bures:** Conceptualization, Validation, Writing, Reviewing. **Nasim Ullah:** Conceptualization, Validation, Writing, Reviewing. **Mohit Bajaj:** Supervision, Visualization, Writing, Reviewing, Editing. **Hossam M. Zawbaa:** Supervision, Writing, Reviewing, Editing. **Salah Kamel:** Supervision, Writing, Reviewing, Editing.

Declaration of competing interest

The authors declare that they have no known competing financial interests or personal relationships that could have appeared to influence the work reported in this paper.

Acknowledgments

The author (Hossam M. Zawbaa) thanks the European Union's Horizon 2020 research and Enterprise Ireland for their support under the Marie Skłodowska-Curie grant agreement No. 847402. The authors thank the support of the National Research and Development Agency of Chile (ANID), ANID/Fondap/15110019.

References

Allouche, A., Etien, E., Rambault, L., Doget, T., Cauet, S., Sakout, A., 2020. Mechanical fault diagnostic in PMSM from only one current measurement: A tacholess order tracking approach. Sensors 20, 5011. http://dx.doi.org/10.3390/s20175011.

Zhao, X., Wang, C., Duan, W., Jiang, J., 2021. Research on sensorless control system of low speed and high power PMSM based on improved high frequency signal injection. Energy Rep. 7, 499–504.

Urbanski, K., Janiszewski, D., 2019. Sensorless control of the permanent magnet synchronous motor. Sensors 19, 3546. http://dx.doi.org/10.3390/s19163546.

Li, Y., Zhao, C., Zhou, Y., Qin, Y., 2020. Model predictive torque control of PMSM based on data drive. Energy Rep. 6, 1370–1376.

Scarcella, G., Scelba, G., Pulvirenti, M., Lorenz, R.D., 2017. Fault-tolerant capability of deadbeat-direct torque and flux control for three-phase PMSM drives. IEEE Trans. Ind. Appl. 53 (6), 5496–5508. http://dx.doi.org/10.1109/TIA.2017.2743070.

Apte, A., Joshi, V.A., Mehta, H., Walambe, R., 2020. Disturbance-observer-based sensorless control of PMSM uing integral state feedback controller. IEEE Trans. Power Electron. 35 (6), 6082–6090. http://dx.doi.org/10.1109/TPEL.2019.2949921.

Alfehaid, A.A., Strangas, E.G., Khalil, H.K., 2021. Speed control of permanent magnet synchronous motor with uncertain parameters and unknown disturbance. IEEE Trans. Control Syst. Technol. 29 (6), 2639–2646. http://dx.doi.org/10.1109/TCST.2020.3026569.

Šmídl, V., Janouš, Š., Adam, L., Peroutka, Z., 2018. Direct speed control of a PMSM drive using SDRE and convex constrained optimization. IEEE Trans. Ind. Electron. 65 (1), 532–542. http://dx.doi.org/10.1109/TIE.2017.2723872.

Xu, W., Junejo, A.K., Liu, Y., Hussien, M.G., Zhu, J., 2021. An efficient antidisturbance sliding-mode speed control method for PMSM drive systems. IEEE Trans. Power Electron. 36 (6), 6879–6891. http://dx.doi.org/10.1109/TPEL.2020.3039474.

Xu, W., Jiang, Y., Mu, C., Blaabjerg, F., 2019. Improved non-linear flux observer-based second-order SOIFO for PMSM sensorless control. IEEE Trans. Power Electron. 34 (1), 565–579. http://dx.doi.org/10.1109/TPEL.2018.2822769.

Mani, P., Rajan, R., Shanmugam, L., Joo, Y.H., 2019. Adaptive fractional fuzzy integral sliding mode control for PMSM model. IEEE Trans. Fuzzy Syst. 27 (8), 1674–1686. http://dx.doi.org/10.1109/TFUZZ.2018.2886169.

Junejo, A.K., Xu, W., Mu, C., Ismail, M.M., Liu, Y., 2020. Adaptive speed control of PMSM drive system based a new sliding-mode reaching law. IEEE Trans. Power Electron. 35 (11), 12110–12121. http://dx.doi.org/10.1109/TPEL.2020.2986893.

Nguyen, A.T., Basit, B.A., Choi, H.H., Jung, J., 2020. Disturbance attenuation for surface-mounted PMSM drives using non-linear disturbance observer-based sliding mode control. IEEE Access 8, 86345–86356. http://dx.doi.org/10.1109/ACCESS.2020.2992635.

Niu, S., Luo, Y., Fu, W., Zhang, X., 2020. An indirect reference vector-based model predictive control for a three-phase PMSM motor. IEEE Access 8, 29435–29445. http://dx.doi.org/10.1109/ACCESS.2020.2968949.

Yang, B., Yu, T., Shu, H., Zhang, Y., Chen, J.J., Sang, Y., Jiang, L., 2018. Passivity-based sliding-mode control design for optimal power extraction of a PMSG based variable speed wind turbine. Renew. Energy 119, 577–589.

Nicklasson, P.J., Ortega, R., Espinosa-Perez, G., 1994. Passivity-based control of the general rotating electrical machine. In: Proceedings of 1994 33rd IEEE Conference on Decision and Control, Vol. 4. pp. 4018–4023. http://dx.doi.org/10.1109/CDC.1994.411573.

Nicklasson, P.J., Ortega, R., Espinosa-Perez, G., Jacobi, C.G.J., 1997. Passivity-based control of a class of blondel-park transformable electric machines. IEEE Trans. Automat. Control 42 (5), 629–647. http://dx.doi.org/10.1109/9.580867.

Achour, A.Y., Mendil, B., Bacha, S., Munteanu, I., 2009. Passivity-based current controller design for a permanent-magnet synchronous motor. ISA Trans. 48 (3), 336_346.

Ramirez-Leyva, F.H., Peralta-Sanchez, E., Vasquez-Sanjuan, J.J., Trujillo-Romero, F., 2013. Passivity-based speed control for permanent magnet motors. Proc. Technol. 7, 215–222.

Khanchoul, M., Hilairet, M., Normand-Cyrot, D., 2014. A passivity-based controller under low sampling for speed control of PMSM. Control Eng. Pract. 26, 20–27.

Wang, R.l., Lu, B.C., Hou, Y.L., Gao, Q., 2018. Passivity-based control for rocket launcher position servo system based on ADRC optimized by IPSO-BP algorithm. Shock Vib. http://dx.doi.org/10.1155/2018/5801573.

Liu, X., Yu, H., Yu, J., Zhao, Y., 2019. A novel speed control method based on port-controlled hamiltonian and disturbance observer for PMSM drives. IEEE Access 7, 111115–111123. http://dx.doi.org/10.1109/ACCESS.2019.2934987.

Ortega, R., Schaft, A.V.D., Maschke, B., Escobar, G., 2002. Interconnection and damping assignment passivity-based control of port-controlled hamiltonian systems. Automatica 38 (4), 585–596.

Ortega, R., Canseco, E.G., 2004. Interconnection and damping assignment passivity-based control: a survey. Eur. J. Control 10 (5), 432–450.

Belkhier, Y., Achour, A.Y., Hamoudi, F., Ullah, N., Mendil, B., 2021. Robust energy-based non-linear observer and voltage control for grid-connected permanent magnet synchronous generator in the tidal energy conversion system. Int. J. Energy Res. 45, 13250–13268. http://dx.doi.org/10.1002/er.6650.

Zakharov, V., Minav, T., 2020. Analysis of field oriented control of permanent magnet synchronous motor for a valveless pump-controlled actuator. Proceedings 64 (1), 1–19.